International Journal of Advanced Technology and Engineering Exploration, Vol 11(118)
ISSN (Print): 2394-5443 ISSN (Online): 2394-7454
http://dx.doi.org/10.19101/IJATEE.2023.10102501

Research Article

Parametric analysis and performance evaluation of piled raft foundations: comparing hollow and conventional systems

Gyan Garima Singh[1*], R.P. Tiwari[2] and Vijay Kumar[3]
Research Scholar, Department of Civil Engineering, MNNIT, Prayagraj, Uttar Pradesh, India, 211004[1]
Professor, Department of Civil Engineering, MNNIT, Prayagraj, Uttar Pradesh, India, 211004[2]
Assistant Professor, Department of Civil Engineering, MNNIT, Prayagraj, Uttar Pradesh, India, 211004[3]

Received: 29-October-2023; Revised: 15-September-2024; Accepted: 18-September-2024

Abstract
Piled raft foundations (PRF) are commonly used in areas with unstable or weak soil conditions, where traditional foundations may not provide adequate support for tall buildings and large structures. Previous studies on PRF assumed that the connecting piles were solid, and the concept of hollow PRF remained unexplored. Nonetheless, the piles that are firmly attached to the raft in this type of foundation system can be regarded as having hollow cross-sections for cost-efficiency. The present research undertakes a comparative analysis of hollow and solid PRF, focusing on square-cross-section piles using finite element analysis (FEA) through Abaqus three-dimensional (3D) software. In this study purely vertical loading up to 1.0 MPa is considered for thorough analysis. In the case of a hollow PRF, the piles are typically hollow, and during the installation process, the empty spaces within the hollow piles in a combined PRF are typically filled with soil material from the surrounding foundation area. As a result, it has found that the pressure settlement behaviour of a hollow PRF with an outer diameter of 1.0 m and an inner diameter of 0.5 m exhibits a similar tendency to that of a solid PRF with the same outer diameter. In this manner hollow PRF represent the more suitable and cost-effective foundation type. This process enhances both strength and stability, while also reducing the amount of material required for casting the foundation.

Keywords
Piled raft foundations, Finite element analysis, Comparative study, Abaqus 3D, Hollow piled raft.

1.Introduction
The construction of skyscrapers began in the late 1970s, marking a significant shift in urban architecture. However, many of these tall buildings were initially supported by shallow foundations, which led to settlement issues that exceeded permissible limits. A notable example is the Deutsche Bank Twin Towers in Frankfurt am Main, Germany, constructed between 1979 and 1984. The towers were built on a simple 80 m × 60 m × 4 m thick foundation slab, where the recorded settlement ranged from 0.10 m to 0.16 m [1]. These challenges prompted researchers to explore alternative foundation solutions. A significant advancement came with the work of researchers [2], who proposed incorporating piles beneath the raft foundation to address settlement issues.

This approach was first implemented in Germany between 1983 and 1985 during the construction of the Messe-Torhaus building in Frankfurt am Main, which utilized a piled raft foundation (PRF). This method, wherein both the raft and piles share the load simultaneously under vertical stress, has since gained widespread acceptance as an efficient and cost-effective foundation solution for tall buildings. The primary advantage of a PRF lies in its ability to distribute loads effectively: the raft provides the necessary bearing capacity, while the piles act as settlement reducers. The placement of piles beneath the raft significantly reduces differential and average settlements, a concept initially proposed by [2, 3] and further refined by other researchers [4–8]. The interaction between the raft and piles in a PRF system plays a crucial role in determining the load-bearing responses, making the consideration of load-sharing features essential in PRF design, as emphasized by [9, 10]. Over the years, numerous analytical techniques, design concepts, and recommendations have been

*Author for correspondence

developed for PRF under vertical stress. These include simplified analysis approaches [8, 11], analytical techniques [12], and rigorous numerical methods [13–15]. Studies by [16, 17] have also provided valuable insights into the economic and cost-effective design criteria for PRF. The evolution of PRF design philosophies, including conventional theory, creep piling theory, and the control of differential settlements, has been thoroughly demonstrated by [8].

In the conventional approach, foundations were designed as a group of piles supporting most of the loads from the superstructure, with a small portion distributed to the underlying soil via a cap. This method often required a high factor of safety, as the working loads were significantly less than the maximum bearing capacity of the soil. Conversely, the creep piling method involves operational loads that are closer to the ultimate bearing capacity, typically reaching 70%-80% of the failure load. This method, initially intended for soft cohesive soils, uses a raft and piles to minimize overall settlements. The third design philosophy involves strategically placing piles under the raft to reduce differential settlements. Further advancements in PRF design include the work of [18], who reported on the optimal micro-pile design for concrete square footings reinforced with micro-piles using the PLAXIS program, demonstrating a significant increase in bearing capacity.

Most studies have focused on solid piles within PRF systems, with limited exploration of hollow piles. This study is motivated by the need to bridge this research gap by conducting a comparative analysis of hollow and solid PRF. The objective is to evaluate the suitability of hollow piles for improving load distribution, enhancing structural integrity, flexibility, and ease of construction in foundation systems.

This paper advances current research by introducing a detailed numerical modelling approach for PRF systems, grounded in extensive literature. It also provides new insights into the design and optimization of hollow PRF, offering a fresh perspective on this emerging concept.

The manuscript is organized as follows: Section 2 reviews the literature on PRF numerical modelling development. Section 3 discusses the methods adopted in this study to support hollow PRF. Section 4 presents the results and their interpretation, while section 5 includes the discussion on study's key findings and finally section 6 concludes and also provide recommendations for future research.

2.Literature review

PRF comprises a platform, or raft, supported by both the soil and deep-seated piles drilled into the ground underneath. This combination of soil and pile support makes PRF a viable and cost-effective alternative foundation system for large buildings, effectively preventing settlement and enhancing bearing capacity, as indicated by [19]. The raft guarantees even distribution of the load in the soil, while the piles offer vertical support by transferring the load to deeper and stable soil layers. The stiffness of these components – raft, pile, and soil – significantly influences how the overall load is distributed within a PRF. In a study presented by Jeong et al. (2024) [20] introducing an enhanced analytical method, MEGA piles, for analysing the load distribution and deformation of rafts and PRF, considering raft-pile flexibility and soil-pile nonlinearity. Through numerical analyses and validation against other methods and field data, it demonstrates improved prediction accuracy for PRF load sharing and settlement behaviour. A study investigates the load-sharing mechanism in PRF through numerical studies, aiming for optimized design. Using finite element analysis (FEA) in PLAXIS three-dimensional (3D), it explores the load-sharing ratio across various parameters such as pile spacing, length, raft settlement, and base depth. Results demonstrate significant increases in load-sharing ratio with higher pile spacing, settlement, and raft base depth, and decreased pile numbers. The study introduces stiffness modification ratios and reveals a master curve that unifies key parameters, providing insights for controlling the load-sharing mechanism effectively [21]. Circular PRF, employing a circular distribution of piles, typically exhibit minimal differential settlements [22]. Factors such as geometry, size, interactions, and material properties (concrete, steel, or soil type) affect the stiffness of each element. In the scenario of medium to dense sand conditions, choosing a PRF with fewer number but larger diameter and length piles is more beneficial than opting for a PRF supported by numerous piles with smaller dimensions, as suggested by Bhartiya et al. (2022) [23]. Nevertheless, when confronted with loose sand, it is advisable to opt for a PRF arrangement that incorporates a greater number of piles to reduce the potential for individual pile capacity failure. In a literature [24], it is investigated that the performance of a medium embedment depth PRF in soft soil through numerical modelling and parametric study. It examines the effects of foundation geometry and stiffness ratio on performance, analyses failure mechanisms, and proposes analytical and semi-empirical models for prediction. Findings highlight the

significant influence of pile spacing on ultimate carrying capacity, with a failure mechanism involving both bearing and shear at the base and sides of the pile group, particularly on hyperbolic planes. A study utilises 3D FEA to investigate the long-term behaviour of PRF on clayey soils, validated with field test outcomes. Numerical results show that the load-sharing ratio in PRF increases by 34–48% with increasing number of piles, 6–19% with increasing pile diameters (D), and 11–20% with increasing raft widths. The research also analyses consolidation settlement factors, proposing expressions and a design equation validated through numerical examples, offering valuable insights for PRF design [25]. Under combined loading conditions, the lateral capacity of a PRF exhibits an increase compared to its individual capacity, as indicated by references [1, 26]. Chanda et al. (2023) [27] reviews contemporary research on PRF under lateral loading, aiming to address gaps in design provisions. It emphasizes soil-structure interaction (SSI) in seismic design and discusses important aspects such as load-sharing, bending moment, peak acceleration, and deformation. Case studies on PRF performance under seismic conditions are also examined, offering valuable insights for developing design guidelines under lateral loading in various subsoil conditions. Because of the influence of raft-to-pile contact, the load responses and transfer of loads relation of piles of PRF differ from that of single pile [28]. In the realm of supporting pseudo-static seismic loads, a PRF surpasses a group pile foundation, as noted by [29]. Researchers [30–32] have developed a 3D numerical model using FE software to evaluate the performance of PRF under various parametric combinations and soil properties. Researchers [33] presents a simplified method utilizing the Vlasov model for nonlinear analysis of PRF under vertical loads, offering a cost-effective solution for low to medium-rise buildings on weak soils. The analysis involves modelling the raft as a thin rectangular plate and representing the granular layer and piles as nonlinear springs according to the Vlasov model. Comparison with existing 3D FEA results demonstrate the method's effectiveness in predicting PRF behavior. A parametric study explores the impact of various parameters, aiding in achieving economical PRF designs. In pile groups with unequal lengths, there is a significant increase in lateral shear at the pile head compared to symmetric arrangements, irrespective of the input motion [34]. This heightened shear force results from the additional force generated by the asymmetry, leading to torsional vibrations in higher modes. This, in turn, causes a higher shear force at the pile head in asymmetric cases. Have proposed a new prediction model and simplified expressions to assess load-sharing responses, interaction behaviours, and factor of safety calculations, incorporating the serviceability requirements of different structures [35–37]. For accurate settlement estimates, analytical methods must appropriately consider the nonlinear behaviour of piles and interactions between the raft and soil, pile and soil, PRF and soil [38]. Furthermore, Samanta and Bhowmik (2019) [39] have conducted a PRF analysis using a 3D numerical technique in soft soil, enhanced with the application of stone columns. Researcher focuses on the parametric analysis of PRF, assessing the impact of various design parameters on structural and geotechnical aspects. It examines settlement, raft-soil contact behaviour, bending moment, axial stress on piles, and soil stress in different directions. Results indicate that adding piles under the raft controls differential settlement, while normalized differential settlement increases with the pile spacing to diameter ratio (S/D). Raft width affects contact pressure, with a higher number of piles causing a more prominent increase, and increasing S/D ratio leads to higher bending moments [40]. FEA is used to explore various parameters' effects, including helix plate diameter, number, and pile spacing, on helical piled raft foundation (HPRF) performance in a cohesionless soil medium. Results indicate that HPRF exhibits lower ultimate settlement and higher tensile capacity than PRF, with helix diameter and pile spacing playing significant roles. The study provides valuable insights for optimizing HPRF design for improved settlement and tensile performance [41]. A field load tests conducts on both a single pile and a 2 × 2 pile group in a PRF, considering the time effect. It monitors settlement, axial load on piles, shaft friction, moments in the raft, and load sharing ratio during gradual compressive loading. Nonlinear analyses, including an approximate procedure based on the theory of interaction factor and a simplified method considering time effects, are suggested and validated with field results. Parametric studies assess immediate and time-dependent settlements by varying pile parameters and configurations, indicating a reduction in settlement compared to measured values [42]. Roh et al. (2019) [43] investigated the settlement of PRF and load-sharing behaviour, considering the effect of groundwater. The results indicate a decrease in settlement values with groundwater level, with minimal impact on load-sharing ratios. A study conducted by [44] in Joo Pessoa, Brazil, investigated the use of hollow auger piles in PRF designs.

The studies reviewed have focused on various aspects of PRF, primarily involving solid piles. Research has

investigated load-sharing mechanisms, settlement behaviour, and structural performance under different loading conditions. Numerical modelling and FEA have been used to explore factors such as pile spacing, raft flexibility, and soil-pile interactions. Some studies have introduced simplified analytical methods and models for predicting PRF behaviour, while others have conducted field tests to validate theoretical findings. Limited research has addressed hollow piles, with recent studies beginning to explore their potential benefits.

Most studies in this field have concentrated on solid piles within PRF, with limited attention given to hollow piles. Research has primarily focused on optimizing cost, load distribution, structural integrity, flexibility, and construction ease. To address this gap, comparative analyses have begun to evaluate the performance of hollow versus solid PRF, assessing their effectiveness in enhancing load distribution, structural integrity, and overall design flexibility.

3.Methods

3.1Input parameters

As symmetry is present in the model, the quarter model of the combined PRF is set up in the present work for simple analysis. The size and positions of the piles, the thickness and plan dimensions of the raft, and the dimensions and borders of the soil block are all accurately laid down in the pile, raft, and soil model. The components of the PRF model are then given material property specifications and applied to them. The parts of the PRF models (soil block and PRF) are both properly and correctly assembled. The model must be run in two stages, thus two steps are generated and fixed to execute the model at appropriate increments. The beginning and maximum increment sizes are maintained at 0.1 and 0.1 for step-1 and 0.05 and 0.1 for step-2, respectively. The minimum increment size in both the steps are set to 10-10 and the maximum number of increments are 105. Two types of interaction properties are created for assigning the contact surface between PRF and soil interfaces. The interfaces are frictionless in step-1 and frictional contact are assigned in second step having a friction coefficient 0.4 between the master (rigid PRF) and slave surfaces (flexible soil). In solid PRF having 2×2 configuration, a total of 6 contact pairs have been generated, on the other hand, in hollow PRF with same configuration, a total of 15 contact pair have been generated. Predefined field are defined in initial step for simulating the self-weight of the foundation and soil modelled. Then, the model is applied with all the boundary conditions and loads are applied in two stages. In stage-1 gravity loading applied and in second stage uniformly distributed loads acts over the top surface of raft.

3.2Hollow and solid PRF configurations

Hollow PRF is a variation of the traditional PRF where the piles are hollow and can be used to improve the drainage and ventilation of the soil underneath the foundation. In the present study, square cross-section hollow and solid PRF are analysed. The spacing to width ratio (S/B ratio) is taken 5 and 10 for solid PRF having width 1.0 m and 0.5 m respectively and 5 for hollow PRF. The raft dimension is chosen 10 m × 10 m as according to [45]. The raft soil stiffness is given by Equation 1 as per [9] and the chosen raft soil stiffness in present study is 0.0295 corresponding to thickness of raft 0.5m.

$$k_{rs} = \frac{4E_r B t_r^3 (1-\vartheta_s^2)}{3\pi E_s L_r^4 (1-\vartheta_r^2)} \quad (1)$$

According to [13], 2×2 square cross-section piles are utilised in present study. The raft is elevated above the ground, and according to Jeong S. et. al. (2024) [20], the length of the piles is assumed to be 16 m. The detailed geometrical parameters of the hollow and solid PRF models are listed in *Table 1*. The schematic representation of PRF with hollow piles, soil continuum & geometry and combined system of full model of hollow PRF system is shown in *Figure 1*.

Table 1 Hollow and solid PRF parameters used in present study

Parameters (unit)	Symbol	Hollow PRF	Solid PRF
Shape of pile cross-section	-	Square	Square
Length of piles (m)	L_r	16	16
Inner Width of piles (m)	b	0.5	-
Outer Width of piles (m)	B	1.0	0.5, 1.0
Spacing of piles (m)	S	5	5
Number of piles	n	4	4
Shape of raft cross-section	-	Square	Square
Thickness of Raft (m)	t_r	0.5	0.5
Cross-Section of Raft	-	10m x 10m	10m x 10m
Soil Block Size	-	40m x 40m x 25m	40m x 40m x 25m

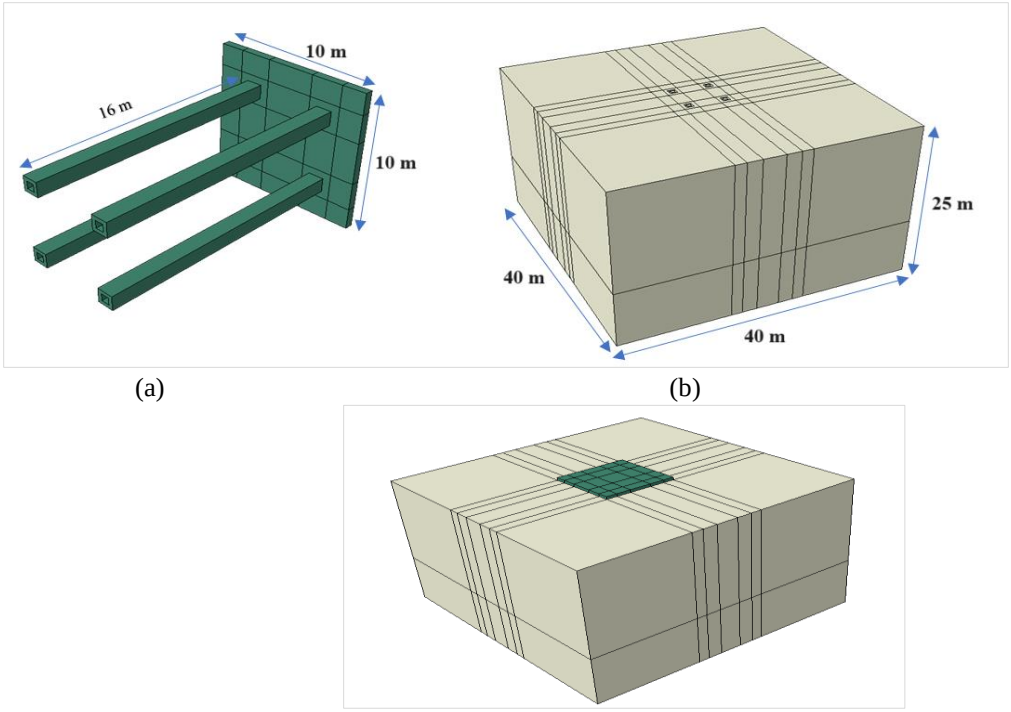

Figure 1 Schematic representation of hollow PRF system a. PRF with hollow piles b. soil continuum & geometry, c. combined system of full model of hollow PRF system

3.3 Numerical analysis

FEA software enables engineers to simulate the interactions between raft, piles, and soil capturing their behaviour accurately. This section explores the complexities of finite-element modelling for both hollow and solid PRF, elucidating the process through a detailed flow diagram depicted in *Figure 2*. The numerical analysis process begins with the development of a FE model using ABAQUS, where the geometry of the raft, piles, and surrounding soil is defined, followed by assigning material properties and interaction characteristics to simulate real-world conditions. After constructing the model, it undergoes validation by comparing its results with experimental or field data. If discrepancies are found, the model is refined iteratively until it accurately reflects observed behaviour. Once validated, the model is applied to analyse the performance of a PRF in sandy soil, focusing on key parameters like load distribution and settlement behaviour. Finally, the results are thoroughly analysed to gain insights into the PRF' effectiveness under various conditions.

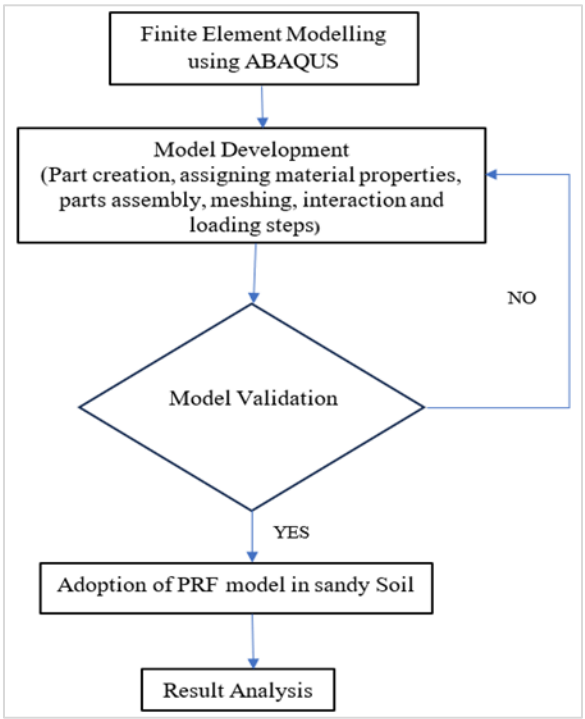

Figure 2 Finite-element modelling process for PRF soil-foundation interactions: flow diagram

3.3.1 Finite element modelling and boundary conditions

The behaviour of all the hollow and solid square PRF is investigated using 3D FE model in complete Abaqus environment (Abaqus/CAE) software in accordance with [46]. The entire model of PRF is a combination of concrete raft, network of piles, soil block and the interaction of soil with foundation structure on the interfacing of PRF and soil. The width of the piles in solid PRF are 0.5 m and 1.0 m and the outer and inner width of hollow PRF is 1.0 m and 0.5 m respectively. The piles are of 16 m length spaced 5 m apart throughout the analysis as discussed above. While assessing the performance of PRF, studies have found significant border effects. Due to which, the soil continuum underwent a first elastic and elastic-plastic analysis with various soil widths and depths. The soil boundaries for PRF models were chosen as 4B (where B is foundation width) in accordance with the preliminary findings, and a depth of 2.5B was decided to avoid any boundary effect as reported in [47]. Meshing was done using 8-node linear brick element (C3D8R element) for reduced integration and hourglass control. From a convergence study, the total number of elements obtained are 996 and 39880 for PRF and soil block respectively. The 3D FE discretized mesh and the boundary conditions of a hollow PRF as the soil domain's side boundaries are constrained horizontally, while its bottom boundaries are constrained in both horizontal and vertical directions as shown in *Figure 3*. To account for the impacts of bending, the raft is meshed using FE elements so that it has a minimum of two elements running along its thickness direction. The 3D analysis of a pile raft often takes a long time to compute as the number of element and nodes rises. In this regard, the soil mesh is discretized in the model so that it is finer close to the piles and gently gets coarser farther away. The aspect ratio of the elements was maintained in reasonable range during this process within the allowable range to ensure the program's successful operation and to reduce the numerical error. Compressible layer base is placed 25 m below the surface of the ground [34], and the model extends 40 m in the horizontal direction. The far field border is regarded as being 15 m away from raft edge. At the soil domain's base, all degrees of freedom are constrained. The outer side walls are on rollers, which means that horizontal direction movements are constrained but not those in the vertical direction. The piles to be assumed in a stress-free condition at the beginning of the research because modelling a pile placement procedure is somewhat complex. The present analyses do not take in to account the change in soil stress during pile placement.

3.3.2Material properties and constitutive model

The constitutive model choice for soil and properties of material for the PRF rely on type of loading, soil conditions, and complexity of the throughout analysis. The Drucker-Prager model, Mohr-Coulomb model, Cam-Clay model and modified Cam-Clay model are few examples of the various constitutive models that can be used for simulating the actual soil behaviour. These models can capture the nonlinear behaviour of soil, including plastic deformation and strain softening, but all these models may be complex due to presence of additional parameters. A total of nine parameters governs the Drucker-Prager criterion and in similar ways Cam-Clay model is also somewhat complex. In the present study, Mohr-Coulomb plasticity model has been utilized for governing the plasticity of the foundation soil block, which is regarded as an elastic completely plastic material as suggested elsewhere in [34]. For the analysis, it is necessary to specify the soil's elastic modulus, poison's ratio, density, and shear strength parameters like friction angle and cohesion which are referred from [48]. For the soil, a 0o angle of dilatancy is considered as suggested in [37], but if we proceed with 0º for angle of dilatancy in Abaqus software it shows an error, to overcome this error very small value of angle of dilatancy of 1º was considered in present study. *Table 2* lists all of the specific soil (sand) and foundation material (concrete) characteristics that were employed in this research work. Pile material can be modelled using linear elastic or nonlinear beam or shell elements. The constitutive models can capture the pile's axial, bending, and shear behaviour. The raft can be modelled using linear elastic or nonlinear shell elements. The constitutive models can capture the raft's bending and shear behaviour. Concrete of the M30 grade with an elastic modulus of $E = 5000 \sqrt{fck}$ (IS-456 2000), where fck is the concrete's compressive strength in MPa, is used to properties of the raft and the piles. The Poisson's ratio, unit weight and modulus of elasticity(E) of concrete that is used for simulating the material of PRF part is taken as reported by [27].

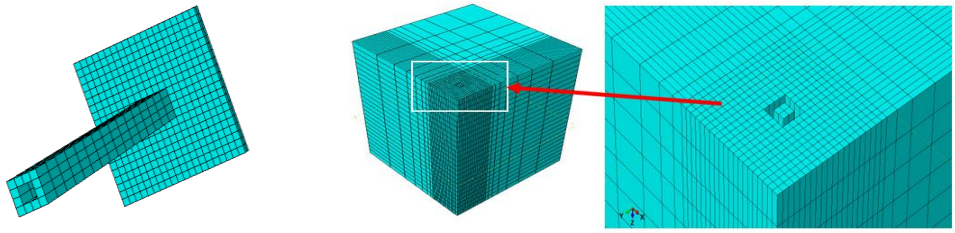

(a) (b) (c)

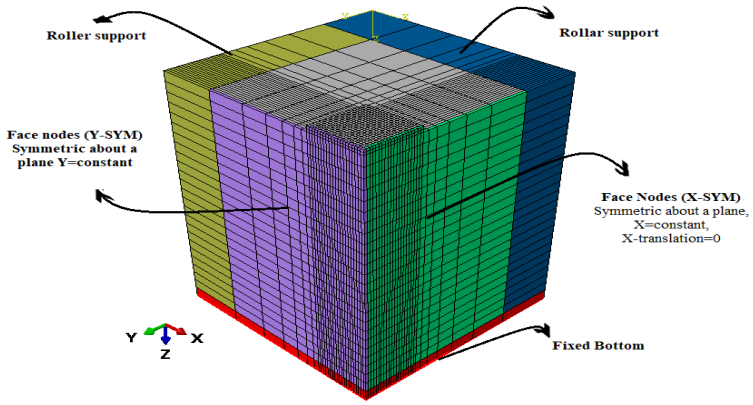

(d)

Figure 3 Illustrative representation of a. Discretized mesh of hollow PRF b. Discretized mesh of soil continuum c. Zoomed view of soil mesh area just below the location of PRF d. Boundary conditions

Table 2 Properties of materials used for numerical modelling

Properties↓	**Symbol**	**Unit**	**Sand**	**Concrete**
Unit Weight	γ	kN/m²	16	24
Modulus of elasticity	E	Mpa	45	2.7386×10^4
Poisson's Ratio	ϑ	-	0.35	0.2
Angle of internal friction	ϕ	-	30º	-
Angle of dilatancy	δ	-	1º	-
Cohesion yield stress	c	kN/m²	0.001 (negligible)	-
Absolute plastic strain	e	-	0	-

3.3.3 Settlement calculations

The vertical settlement of PRF is typically assessed through average settlement, as defined in Equation 2 suggested by [49].

$$S_{avg} = (2S_{center}+S_{corner})/3 \quad (2)$$

where, S_{center} is the Settlement at centre of the raft and S_{corner} is settlement at corner point of raft. According to Equation 3, the differential settling of the raft is calculated [10],

$$S_{diff} = S_{center} - S_{corner} \quad (3)$$

The settlements of the PRF system were elucidated in terms of average settlements, S_{avg} & differential settlements, S_{diff} considering Equation 2 and Equation 3.

3.3.4 Interactions

The master-slave concept, where the stiff surface (pile and raft surfaces) is typically treated as the master surface and the flexible surface (soil surface) as the slave surface, is used to depict the interaction between the three components of the PRF system, i.e., the pile, raft, and subsoil. The separation between a pile and the soil surface is permitted when symmetric general contact modules are used. In this situation, zero thickness slip components transmit shear forces over the surface while compressive forces are present. So, both compressive and shear forces are conveyed between these components. The Coulomb's friction theory governs the connection between shear forces and normal forces at contact surface of pile and soil as reported by [50]. The interface friction phenomenon between concrete foundation and soil surface is set as

frictionless in first stage and frictional during second stage. For the strength mobilisation at pile-soil and raft-soil interfaces, the present study utilises Rinter values for the calculation of interface factor. Rinter was calculated based on the assumption of $\delta = 0.96\ \phi$, Rinter=tan δ, as per [51]. In order to model the PRF to soil continuum interaction, surface to surface type interaction is selected having frictional boundary between master surface and slave surfaces. Here, the key variables that are employed throughout the entire study are explained.

4.Results

4.1 Model validation

In order to ensure the accuracy and reliability of the numerical simulations performed in this research, it is essential to validate the software model used. In this study, the software model was validated against the findings presented in the study conducted by [32]. They investigated the behaviour of PRF subjected to uniformly distributed surcharge loads over the raft's top surface, which is directly relevant to the scope of this research. They conducted a parametric investigation by altering the raft thickness, D, pile length, and distance between piles. They also varied the soil parameters. For pile length variation, tests were carried out in their study using piles that were spaced at a 6D apart and had lengths of 5, 10, and 15 metres. The results for model having 10 m pile length are selected for validation of the software model of the present study. For validation purposes, the identical material properties as mentioned in [32] research study were taken into consideration. *Figure 4* illustrates the comparisons between the findings of the referred study and the present numerical model. The results from the two scenarios are remarkably similar, demonstrating the validity and accuracy of the numerical model developed for this study.

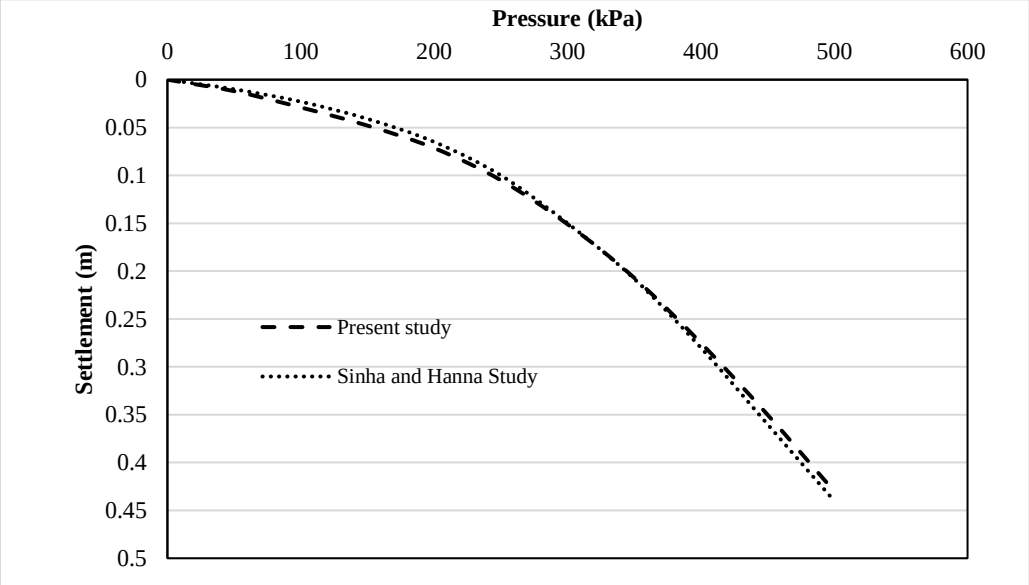

Figure 4 Model Validation graphs showing pressure-settlement curves at central point top of the raft

4.2 Visualisation of deformation contours

Using Abaqus software, 3D FE simulation of a 2×2 PRF systems were run. This study examines the stress and settlement behaviour of pile foundations with solid and hollow piles taking into considerations the interactions between the pile, the soil, and the raft under a static vertical load. Also, the time-dependent stress variation at critical nodes is thoroughly investigated in section 4.6. The stress and deformation contours extracted from the FE software Abaqus-3D are presented in *Figure 5* and *6*. Red coloured zone represents the zone of maximum stress and maximum settlements and blue coloured zones represents minimum values of stress and deformations.

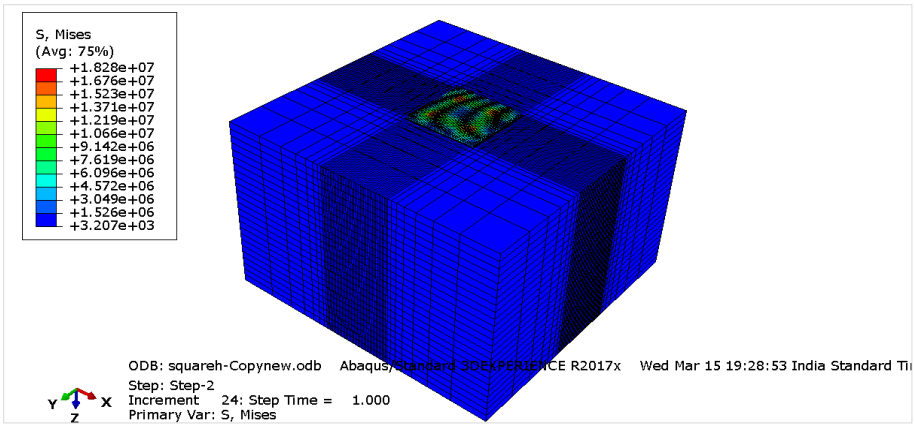

Figure 5 Stress contour of hollow squared PRF extracted from Abaqus software

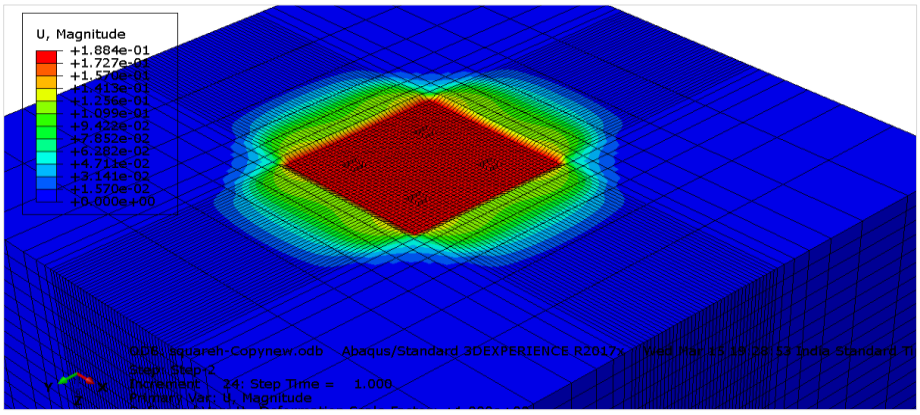

(a)

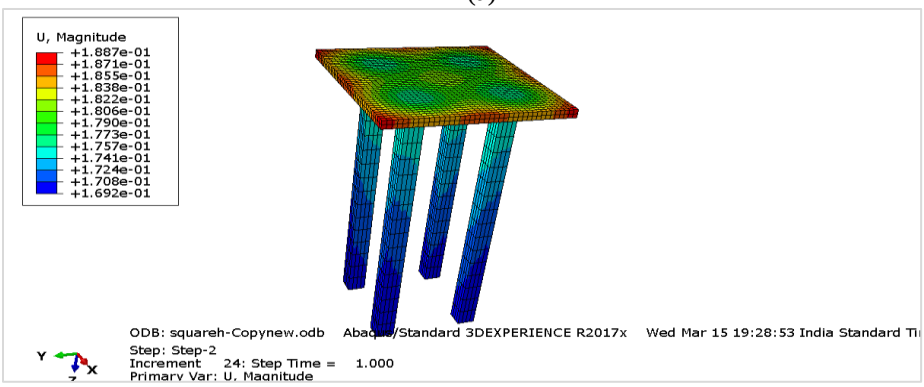

(b)

Figure 6 Stress contour of individual components of hollow squared PRF extracted from Abaqus software a. Soil continuum stress contour b. Hollow PRF stress contour

4.3 Average settlement analysis

In the present investigations, settlement analysis of hollow and solid PRF has been examined to record the degree of settlement that may occur owing to the loads imposed on the foundation system. Abaqus-3D investigations at the central node of the foundation soil were used to capture the pressure settlement variations in both types of foundation models. *Figures 6* and *7* depict the settlement profile contour for solid square PRF with widths of 0.5 m and 1.0 m and hollow square PRF with inner and outer pile widths of 0.5 m and 1.0 m, respectively, as generated from data extracted from the Abaqus-3D programme. Typically, foundation soil or another lightweight material is placed inside the

hollow core between the piles to lower the weight of the foundation and the amount of material needed to build it. This means that the engineers can complete their project while utilising less material by economically substituting hollow PRF for solid PRF in the integrated PRF projects. *Figure 7* and *Figure 8* display the settlement profiles of solid PRF and hollow PRF with an outside diameter of 1.0 m. It is simple to observe that the greatest settlement recorded for a hollow PRF is 0.1887 m, which is quite comparable to the settlement recorded for a solid PRF (0.1879 m). The graph in *Figure 9* makes it clear that the pressure settlement behavior of a hollow PRF with an outer diameter of 1.0 m and an inner diameter of 0.5 m exhibits a similar tendency to that of a solid PRF with the same outer diameter.

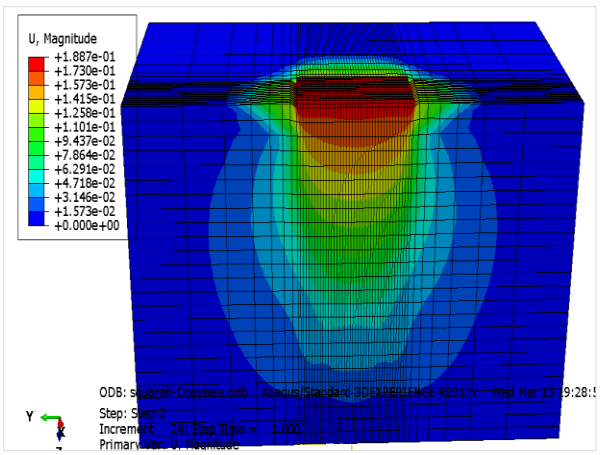

Figure 7 Deformation Contour of hollow PRF

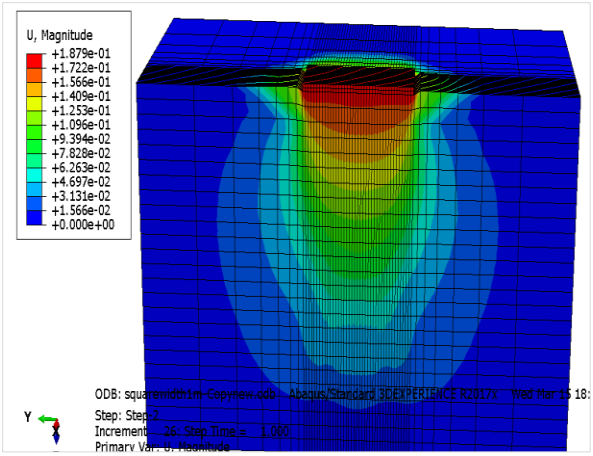

Figure 8 Deformation Contour of Solid PRF, B=1.0m

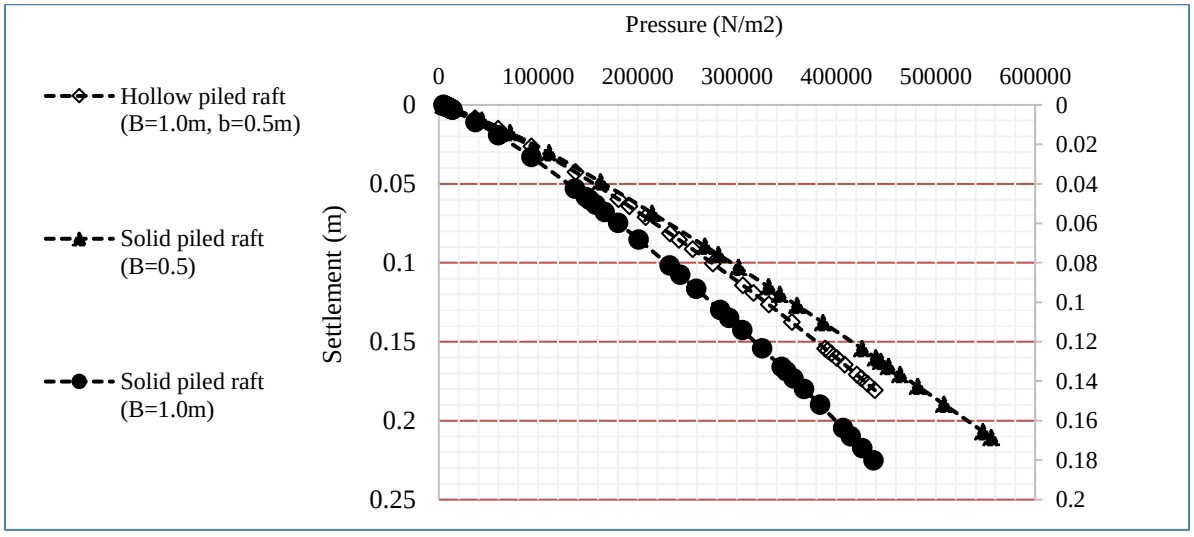

Figure 9 Pressure-Settlement Curves for hollow and solid PRF in present study

Overall, it can be said that, hollow PRF can provide effective solutions for reducing settlement because these foundations are more economical that solid PRF. The choice of foundation type depends on a range of factors, including the site conditions, the structural design, and the available construction materials and methods. Careful analysis and design are critical to ensure that the foundation system is properly sized and configured to withstand the anticipated loads and minimise settlements.

4.4 Differential settlement analysis

The square PRF with solid piles having widths of 0.5 m and 1.0 m and hollow PRF with inner and outer widths of 0.5 m and 1.0 m have been investigated for differential settlement with all other specifications staying the same. Equation 2 is used to compute the differential settlements of the raft component of the

PRF employed in this study. These settlements are then plotted against pressure at the corner and centre of the raft's bottom. *Figure 10* makes it clear that the highest value of differential settlement for a solidly PRF with a width of 0.5 m is recorded as 0.00863 m. In solid PRF with 1.0 m in width and hollow PRF, as stated above, the differential settlement variation with corner and center pressure of the raft's bottom is remarkably similar. *Figures 10* and *11* display the differential settlement variation in the hollow and solid PRF explained above. The highest differential settlement value for a solid PRF with a 1.0 m width is 0.00675 m, and for a hollow PRF, it is 0.00709 m, which is nearly the same. This means that, because they are more affordable, hollow PRF may be a better option than traditional PRF.

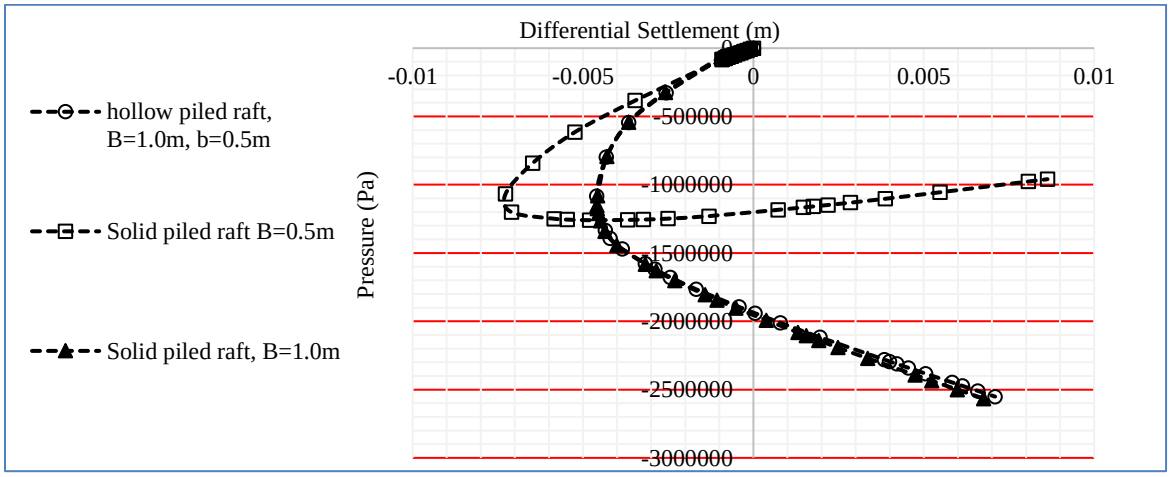

Figure 10 Pressure-differential settlements curves (Pressure at centre point of the bottom of the raft)

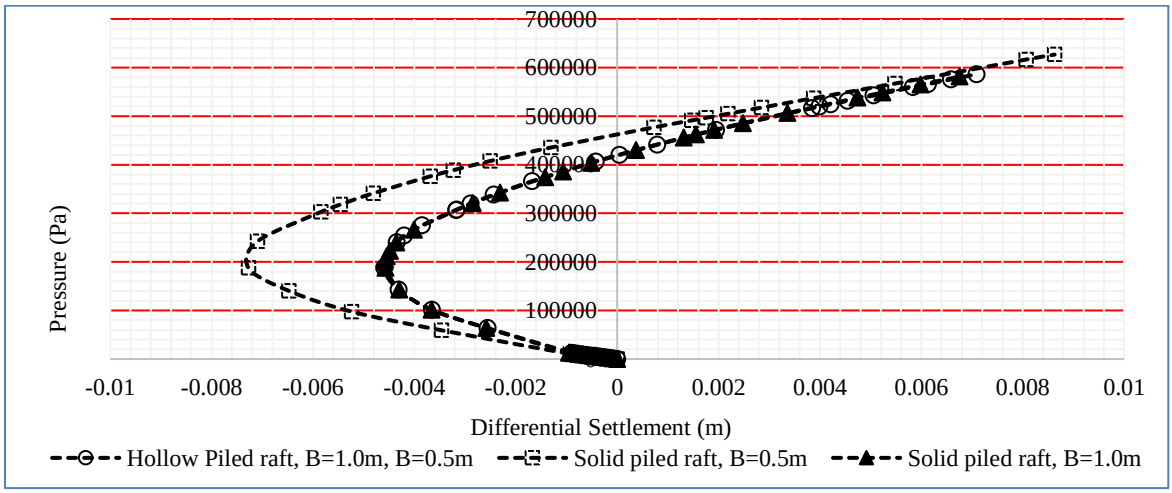

Figure 11 Pressure-differential settlements curves (Pressure at corner point of the bottom of the raft)

4.5 Parametric study

For parametric study, the effect of variation in length to diameter ratio (L/D ratio), D and S/D ratio on average and differential settlement ratios for different pile group to raft width ratios (W_g/W_r) are presented. The average settlements ratio (λ_{avg}) and the differential settlements ratio (λ_{diff}) measure the ratio of PRF's average settlement to that of unpiled rafts and the ratio of PRF's differential settlement to that of unpiled rafts respectively.

The behaviour of a PRF with L/D ratios of 8, 12, and 16, with piles spaced at S=5D, was analysed to understand the effect of L. The effect of varying L/D ratios on λ_{avg} and λ_{diff} for different W_g/W_r ratios is shown in *Figure 12 (a)* and *(b)*. These figures demonstrate that, regardless of the W_g/W_r ratio, λ_{avg}

decreases as L/D increases. This decrease is attributed to the increase in skin friction associated with higher L/D ratios, leading to reduced settlement. Particularly, at a larger W_g/W_r ratio of 0.6, the decline in λ_{avg} is more pronounced, as depicted in *Figure 12 (a)*. To minimize λ_{avg}, it is therefore advisable to incorporate more piles with longer lengths. *Figure 12 (b)* reveals that, across all W_g/W_r ratios, λ_{diff} decreases as the L/D ratio increases, albeit with varying patterns compared to λ_{avg}. While λ_{diff} decreases with increasing L/D for W_g/W_r ratios of 0.3, 0.4, and 0.5, it exhibits an increase at W_g/W_r =0.6. This implies that as the W_g/W_r ratio is raised from 0.3 to 0.5 for a PRF of a given D, λ_{diff} decreases; however, it rises when the ratio is further increased to 0.6.

The study investigated the influence of D on a PRF with a 2×2 pile arrangement, ranging from 0.4 m to 1.6 m. For a W_g/W_r ratio of 0.6, the average settlement (λ_{avg}) demonstrated a rapid decrease with increasing D, particularly up to 0.6 m, after which the trend stabilized, as shown in *Figure 12 (c)*. This behaviour was consistent across different W_g/W_r ratios, with minor variations. Beyond a D value of 0.7 m, the rate of decrease in λ_{avg} with increasing D appeared to reach a plateau, suggesting a potential maximum stiffness of the PRF structure at this D. Regarding λ_{diff}, *Figure 12 (d)* depicted a decrease with increasing D, up to 0.8 m, beyond which λ_{diff} remained constant. The rate of decrease in λ_{diff} with increasing D seemed to vary with the W_g/W_r ratio, showing a diminishing trend as the ratio decreased from 0.6 to 0.4, and from 0.4 to 0.2. This observation implies that the PRF system might have achieved its maximum stiffness at a D of 0.8 m, indicating that further increases in D would have minimal impact on λ_{diff}.

To examine the impact of S/D ratios, the study considered values ranging from 2 to 20 to analyse variations in both λ_{avg} and λ_{diff}. *Figure 12(e)* and *(f)* illustrates the effects of different S/D ratios on λ_{avg} and λ_{diff} for various W_g/W_r ratios. In this context, a λ_{avg} value of 1 indicates equivalence in average settlement between the PRF and an unpiled raft. Observing *Figure 12(e),* it's evident that λ_{avg} decreases as the S/D ratio increases across all pile configurations and W_g/W_r ratios. Moreover, the rate of decline in λ_{avg} intensifies with higher W_g/W_r ratios. Typically, the lowest λ_{avg} value for each W_g/W_r ratio is observed around S/D = 4.5–5.5, after which it gradually rises. This suggests that beyond an S/D ratio of 4.5–5.5, the number of piles might be insufficient, causing them to act more independently, thus leading to a rise in average settlement. Therefore, an S/D ratio around 5 could be considered optimal in terms of average settlement. Furthermore, *Figure 12(f)* demonstrates that λ_{diff} decreases initially with increasing S/D ratio for all pile configurations and W_g/W_r ratios until it reaches a minimum value. Subsequently, λ_{diff} begins to increase with further increases in the S/D ratio. A λ_{diff} value of 1.0 indicates that the differential settlement for the PRF matches that of an unpiled raft.

4.6 Stress-time variation at critical points

The critical point of stress contours are corner centre and midpoint of raft of the foundation system. So, the stress patterns at corresponding nodes of the soil block just below these critical points are recorded and stress-time graphs are extracted directly from Abaqus software and are shown in figures. In *Figure 13 (a),* graph for solid PRF having width 0.5 m is plotted in which, N: 32 denotes node of soil just below corner node of raft, N: 48_1 denotes node of soil just below midpoint of the edge of the raft and N: 60 is the central point of the top surface of the soil block. In *Figure 13 (b),* graph for solid PRF having width 1.0 m is plotted in which, N: 27 denotes node of soil just below corner node of raft, N: 51 denotes node of soil just below midpoint of the edge of the raft and N: 48 is the central point of the top surface of the soil block. In *Figure 13 (c),* graph, for hollow PRF having inner and outer width 0.5 m and 1.0 m respectively, is plotted, in which, N: 27 denotes node of soil just below corner node of raft, N: 54 denotes node of soil just below midpoint of the edge of the raft and N: 48 is the central point of the top surface of the soil block. As these graphs are directly extracted from Abaqus software the units corresponding to the axes are not written. All the units considered in Abaqus software are in SI-Units. For solid PRF having 0.5 m width, the stress at node, N: 32 is reaching to a value of 13.6845 kPa and ends at 5.9838 kPa, at the completion of step-1. The stress point in the end of step-2 is reaching to a very high limit, i.e., 99.1898 kPa and ends at 44.3353 kPa. At corner node the stress varies in zig-zag fashion. At node N: 48_1 the stress variation shows an increasing trend. At the end of first step the stress at this node is reaching a highest value of 11.1852 kPa and at the end of step-2, this value is reached to 183.848 kPa. Showing a similar trend as node N: 48_1, the stress at node N: 60 the stress points are reaching to 8.59697 kPa and 373.995 kPa at the end of step-1 and step-2 respectively. As long as step-1 runs the stress values increases at slow rate. But, when the step-1 ends, the stress concentrations start increasing at high rates. For solid PRF having 1.0 m width, the stress at node, N: 27 is reaching to a value of 16.3019 kPa and ends at 6.64844 kPa, at the completion of step-1.

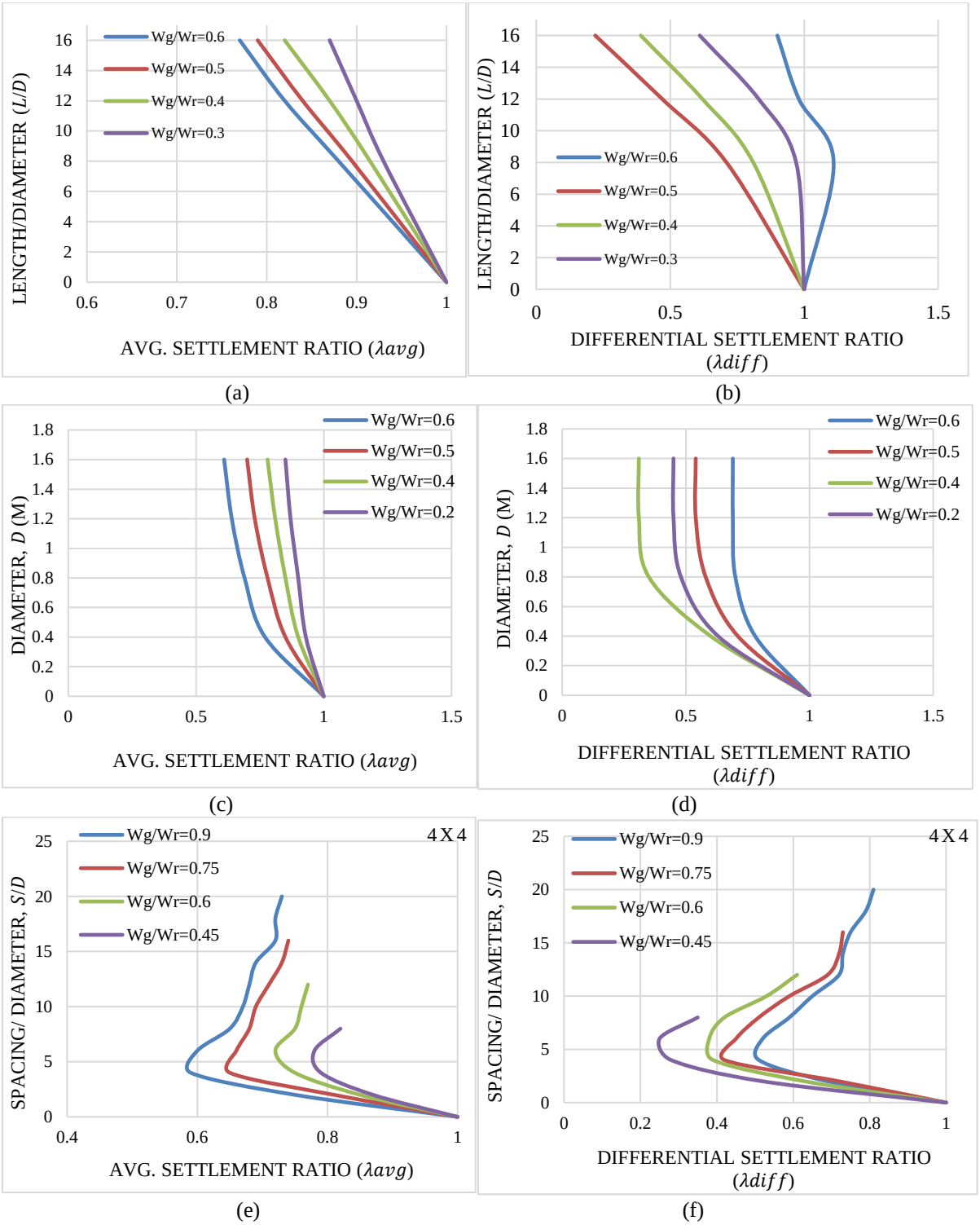

Figure 12 Parametric study of average and differential settlement ratio

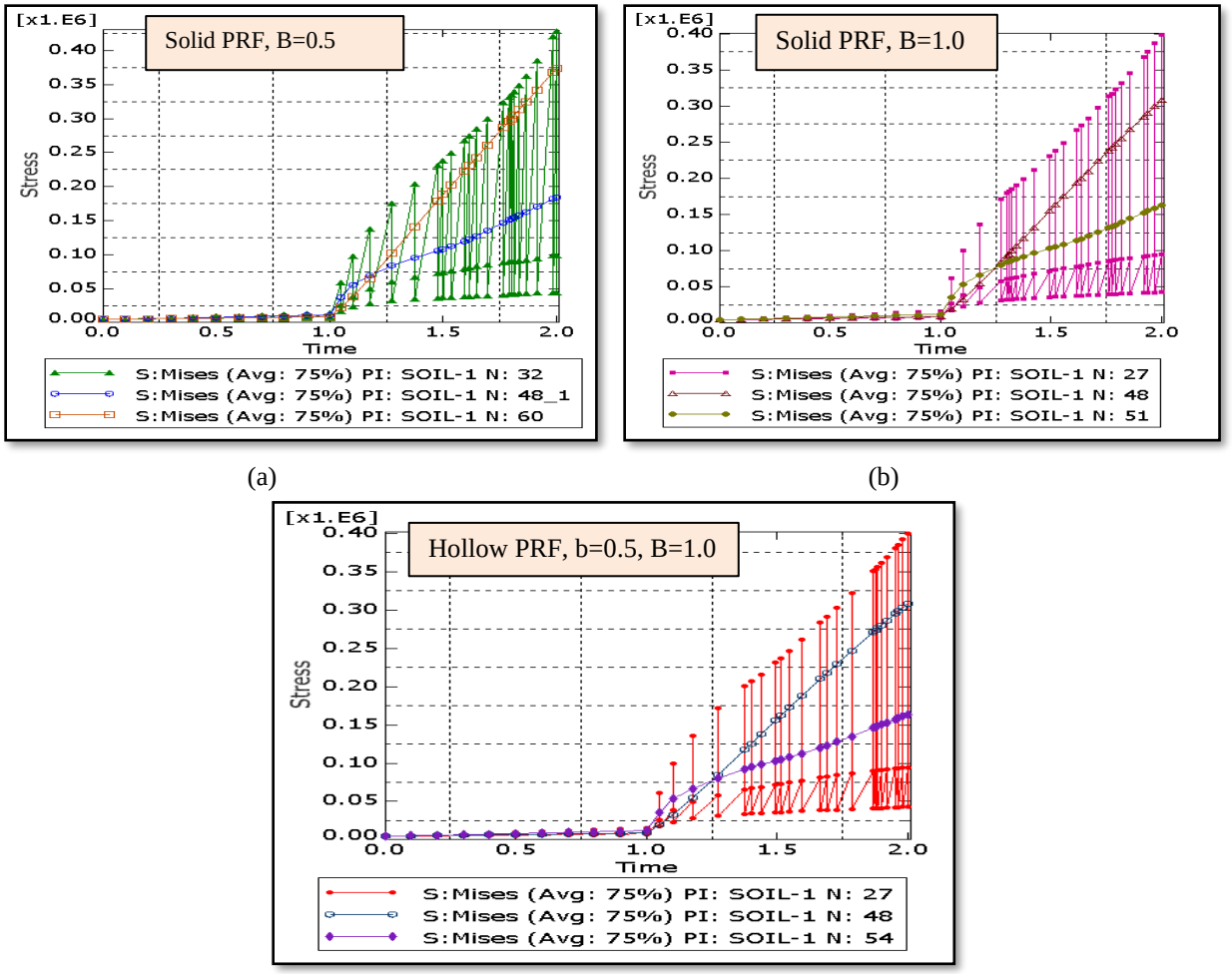

Figure 13 Stress-Time variation at critical notes of foundation soil extracted from Abaqus-3D (a) for solid PRF, B=0.5 m (b) for solid PRF, B=1.0 m (c) for hollow PRF, b=0.5 m, B=1.0 m

The stress point in the end of step-2 is reaching to a very high limit, i.e., 94.5244 kPa and ends at 42.7281 kPa. At corner node the stress varies in zig-zag fashion. At node N: 51 the stress variation shows an increasing trend. At the end of first step the stress at this node is reaching a highest value of 12.4279 kPa and at the end of step-2, this value is reached to 162.803 kPa. Showing a similar trend as node N: 51, the stress at node N: 48 the stress points are reaching to 8.89773 kPa and 307.745 kPa at the end of step-1 and step-2 respectively. For hollow PRF having inner and outer width 0.5 m and 1.0 m respectively, the stress at node, N: 27 is reaching to a value of 9.85568 kPa and ends at 6.499 kPa, at the completion of step-1. The stress point in the end of step-2 is reaching to a very high limit, i.e., 94.5265 kPa and ends at 42.7822 kPa. At corner node the stress varies in zig-zag fashion. At node N: 54 the stress variation shows an increasing trend. At the end of first step the stress at this node is reaching a highest value of 12.0329 kPa and at the end of step-2, this value is reached to 163.333 kPa. Showing a similar trend as node N: 54, the stress at node N: 48 the stress points are reaching to 8.70458 kPa and 308.628 kPa at the end of step-1 and step-2 respectively, which is found to be very much similar to that in solid PRF with width 1.0 m.

The time-dependent stress behaviour of a PRF depends on various factors like soil properties, pile-soil interaction, pile spacing, and foundation loading history. In general, a PRF undergoes both immediate and long-term settlements due to the loads applied to it, and this settlement can lead to time-dependent stress behaviour. In the immediate period after construction, the PRF undergoes primary consolidation settlement due to the compression of the soil. This leads to an

increase in the effective stress in the soil, which causes the soil to consolidate and settle further. The primary consolidation settlement can be calculated using various methods such as Terzaghi's theory, and it is influenced by the soil's coefficient of consolidation and the thickness of the soil layer. In the long-term, the PRF undergoes secondary consolidation settlement due to the viscous deformation of the soil. This settlement occurs over a longer time period and is influenced by factors such as the duration of the load, the magnitude of the load, and the soil's creep behaviour.

5.Discussion

This study presents a comprehensive analysis of both hollow and solid PRF under top surface loading conditions. The investigation began with the validation of a numerical model for solid PRF and extended to compare the performance of hollow and solid PRF. Key parameters, such as D, spacing and length of piles were meticulously examined to derive the conclusions on settlement behaviour. The analysis demonstrated that deformation contours for hollow and solid PRF with the same outer diameter exhibited similar shapes, with only negligible differences in maximum settlement values. Specifically, the maximum settlement for the hollow PRF was recorded at 0.1887 m, closely mirroring the 0.1879 m observed for the solid PRF. Differential settlement across the raft's surface, particularly between corner and centre points, was remarkably consistent between the two types of PRF. This suggest that the overall settlement behaviour of hollow and solid PRF is comparable, providing a basis for considering hollow PRF as a viable, cost-effective alternative in design.

The parametric study reveals that increasing the L/D ratio and D significantly reduces λ_{avg} and λ_{diff} in PRF, with optimal performance observed at an L/D ratio of 16 and a D of 0.7–0.8 m. Additionally, an S/D ratio within the range of 4.5–5.5 appears optimal for minimizing settlement, as further increases cause piles to act more independently, leading to higher settlements. These findings suggest that careful selection of L/D, D, and S/D ratios is crucial for optimizing PRF design to achieve minimal settlements and improved foundation stability.

The stress-time analysis at critical points of the PRF system shows significant stress variations across different nodes. For the solid PRF with a 0.5 m width, the stress at the corner node peaks at 99.19 kPa during step-2, while the midpoint and centre nodes reach 183.85 kPa and 373.99 kPa, respectively. In the solid PRF with a 1.0 m width, the corner node stress peaks at 94.52 kPa, with the midpoint and centre nodes reaching 162.80 kPa and 307.75 kPa. The hollow PRF, with inner and outer widths of 0.5 m and 1.0 m, shows similar patterns, with the corner node stress peaking at 94.53 kPa, and the midpoint and centre nodes reaching 163.33 kPa and 308.63 kPa. These results emphasize the importance of stress distribution in PRF design, especially during critical loading phases.

The results of this study provide valuable insights into the performance of both hollow and solid PRF under top surface loading. The close similarity in maximum settlement values between hollow and solid PRF, despite their structural differences, suggests that hollow PRF can be considered a viable alternative, offering comparable performance with potential cost savings. The parametric analysis highlights the critical influence of L/D ratio, D, and S/D ratio on settlement behaviour, emphasizing the need for precise selection of these parameters to minimize average and differential settlements, thereby enhancing foundation stability. The stress-time analysis underscores the importance of understanding stress distribution across key nodes in the PRF, particularly during critical loading phases, to ensure structural integrity. Overall, these findings advocate for the thoughtful design of PRF, considering both settlement and stress distribution to achieve optimal performance and cost-effectiveness in foundation engineering.

This study implies that hollow PRF can be a cost-effective and sustainable alternative to solid PRF, offering similar settlement performance while using less material. Optimizing key parameters like L/D ratio, D, and S/D ratio is crucial for minimizing settlements and enhancing foundation stability. The findings also indicate the importance of understanding stress distribution to improve the safety and durability of PRF designs, guiding engineers toward more efficient and resilient foundation systems.

Limitations

While the findings are promising, this study has limitations. The numerical model relied on certain simplifying assumptions that may not fully capture the complex behaviour of real-world PRF systems. Factors like soil heterogeneity, pile-soil interaction, and varying loading conditions were idealized, which could affect the accuracy of the results. Additionally, the study focused on a narrow range of parameters, such as specific L/D ratios, D, and S/D ratios, which may not reflect the full diversity of real-world scenarios. The exclusion of lateral and dynamic

loading conditions, as well as potential boundary effects, further limits the generalizability of the findings.

Recommendations

Future studies should aim to address these limitations by incorporating more realistic modelling assumptions, expanding the range of parameters, and considering additional loading conditions. Field validation experiments are also recommended to enhance the robustness and practical applicability of the findings. A comparative study including a wider variety of soil types, pile configurations, and loading scenarios could provide deeper insights into the behaviour of PRF under diverse conditions.

The overall impact of this research is its contribution to advancing PRF design by demonstrating that hollow piles can be a cost-effective alternative without compromising performance. The study provides valuable insights that can guide engineers in optimizing foundation systems, promoting safer, more economical, and environmentally friendly construction practices.

A complete list of abbreviations is listed in *Appendix I.*

6.Conclusion and future work

In this study, a variety of 3D finite-element models were developed to analyse the performance of solid and hollow PRF. A parametric study was performed by varying the L/D ratio, D, and spacing between piles. The stress-strain behaviour was thoroughly examined using the Mohr-Coulomb plasticity model. For the range of soil parameters discussed in this study, the following conclusions can be made:

i. Upon increasing the width of solid PRF from 0.5 m to 1.0 m, there is a decrease in average settlement and differential settlement of the raft by 14.84% and 21.71% respectively.
ii. The maximum value of the pressure reaching at centre and corner point of the bottom of the raft shown to be increased by 103.69% and decrease by 7.228% respectively, when the width of solid square PRF increased from 0.5 m to 1.0 m. This can lead to a conclusion that; central portion of the raft is resisting a good portion of load coming over the top surface of the raft.
iii. The difference in maximum pressure level in Pressure-Settlement curves in only 0.301% and this difference in maximum settlement value is 0.286%.
iv. From Pressure-Differential Settlement curves, the differences in maximum differential settlement levels are observed to be 4.95%, which is also very less, but this difference is somewhat more than that in average settlement and maximum pressure levels.
v. The differences in pressure levels at central and corner points of the bottom of the raft is 0.569% and 0.838%, respectively, which shows the better performance of the hollow PRF because of less material requirements.
vi. Higher L/D ratios resulted in reduced average settlement (λ_{avg}), especially noticeable at elevated W_g/W_r ratios, while λ_{diff} displayed a complex trend. Larger D initially caused rapid declines in both λ_{avg} and λ_{diff}, but these effects stabilized after reaching a certain threshold. Optimal S/D ratios for minimizing settlement were identified around 4.5–5.5, with λ_{diff} reaching a minimum before beginning to increase.

The content outlined in this paper exclusively revolves around FE modelling. In the future, laboratory simulations can be conducted utilizing the developed model or prototype. There may be a variation in soil type, as the sandy soil may be replaced with clay. Also, the parametric study can also be analysed in hollow PRF.

Acknowledgment

The MNNIT, Allahabad, Prayagraj provided the essential support to the authors to complete this study effectively.

Conflicts of interest

The authors have no conflicts of interest to declare.

Data availability

All data supporting the findings of this study are available from the corresponding author upon reasonable request.

Author's contribution statement

Gyan Garima Singh: Conceptualization, modelling, data curation, result analysing, writing – original draft, **R.P. Tiwari:** Conceptualization, reviewing – original draft, supervision. **Vijay Kumar:** Supervision, investigation on challenges and draft manuscript preparation.

References

[1] Chanda D, Saha R, Haldar S. Behaviour of piled raft foundation in sand subjected to combined VMH loading. Ocean Engineering. 2020; 216:107596.
[2] Burland JB, Broms BB, De MVF. Behaviour of foundations and structures. 1978: 495-546.
[3] Fraser RA, Wardle LJ. Numerical analysis of rectangular rafts on layered foundations. Geotechnique. 1976; 26(4):613-30.
[4] Cho J, Lee JH, Jeong S, Lee J. The settlement behavior of piled raft in clay soils. Ocean Engineering. 2012; 53:153-63.

[5] Cooke RW. Piled raft foundations on stiff clays-a contribution to design philosophy. Geotechnique. 1986; 36(2):169-203.
[6] Fioravante V, Giretti D, Jamiolkowski M. Physical modeling of raft on settlement reducing piles. In from research to practice in geotechnical engineering 2008 (pp. 206-29).
[7] Horikoshi K, Randolph MF. Estimation of overall settlement of piled rafts. Soils and Foundations. 1999; 39(2):59-68.
[8] Randolph MF. Design methods for pile group and piled rafts. International Conference on Information and Education Innovations 1994 (pp. 61-82).
[9] Clancy P, Randolph MF. Simple design tools for piled raft foundations. Geotechnique. 1996; 46(2):313-28.
[10] De SL, Mandolini A. Bearing capacity of piled rafts on soft clay soils. Journal of Geotechnical and Geoenvironmental Engineering. 2006; 132(12):1600-10.
[11] Poulos HG. Practical design procedures for design applications of raft foundations. 2000:425.
[12] Clancy P, Randolph MF. An approximate analysis procedure for piled raft foundations. International Journal for Numerical and Analytical Methods in Geomechanics. 1993; 17(12):849-69.
[13] Katzenbach R, Arslan U, Moormann C, Reul OJ. Piled raft foundation: interaction between piles and raft. Darmstadt Geotechnics. 1998; 4(2):279-96.
[14] Poulos HG. Piled raft foundations: design and applications. Geotechnique. 2001; 51(2):95-113.
[15] Ta LD, Small JC. Analysis of piled raft systems in layered soil. International Journal for Numerical and Analytical Methods in Geomechanics. 1996; 20(1):57-72.
[16] Horikoshi K, Randolph MF. A contribution to optimum design of piled rafts. Geotechnique. 1998; 48(3):301-17.
[17] Poulos HG, Davis EH. Pile foundation analysis and design. TRID; 1980.
[18] Haghighy P. Improving the bearing capacity of foundations using micropiles. Elastic. 2017; 2(105):38-46.
[19] Rabiei M, Choobbasti AJ. Piled raft design strategies for high rise buildings. Geotechnical and Geological Engineering. 2016; 34:75-85.
[20] Jeong S, Park J, Chang DW. An approximate numerical analysis of rafts and piled-rafts foundation. Computers and Geotechnics. 2024; 168:106108.
[21] Nguyen NV, Vinh LB, Vo TT. Load-sharing mechanism of piled-raft foundation: a numerical study. European Journal of Environmental and Civil Engineering. 2022; 26(15):7916-31.
[22] Bhartiya P, Basu D, Chakraborty T. Nonlinear settlement of piled rafts in sandy soil. International Journal of Geomechanics. 2021; 21(11):04021214.
[23] Bhartiya P, Chakraborty T, Basu D. Load-settlement response of piled raft foundations in sand. Geomechanics and Geoengineering. 2022; 17(4):1260-83.
[24] Ahmed D, Bt TSN, Ayadat T, Hasan A. Numerical analysis of the carrying capacity of a piled raft foundation in soft clayey soils. Civil Engineering Journal. 2022; 8(4):622-36.
[25] Tarenia K, Patra NR, Rajesh S, Mondal A. Behavior of rigid piled-raft foundation subjected to compressive loading considering time effect: an experimental and analytical study. International Journal of Geomechanics. 2023; 23(12):04023236.
[26] Chanda D, Nath U, Saha R, Haldar S. Development of lateral capacity-based envelopes of piled raft foundation under combined VMH loading. International Journal of Geomechanics. 2021; 21(6):04021075.
[27] Chanda D, Saha R, Haldar S, Choudhury D. State-of-the-art review on responses of combined piled raft foundation subjected to seismic loads using static and dynamic approaches. Soil Dynamics and Earthquake Engineering. 2023; 169:107869.
[28] Kumar A, Choudhury D, Katzenbach R. Effect of earthquake on combined pile–raft foundation. International Journal of Geomechanics. 2016; 16(5):04016013.
[29] Roy J, Kumar A, Choudhury D. Pseudostatic approach to analyze combined pile–raft foundation. International Journal of Geomechanics. 2020; 20(10):06020028.
[30] Mali S, Singh B. Behavior of large piled-raft foundation on clay soil. Ocean Engineering. 2018; 149:205-16.
[31] Modak R, Singh B. A parametric study of large piled raft foundations on clay soil. Ocean Engineering. 2022; 262:112251.
[32] Sinha A, Hanna AM. 3D numerical model for piled raft foundation. International Journal of Geomechanics. 2017; 17(2):04016055.
[33] El-garhy BM. A simplified method for the nonlinear analysis of composite piled raft foundation. Geotechnical and Geological Engineering. 2022; 40(9):4357-75.
[34] Chaudhuri CH, Chanda D, Saha R, Haldar S. Three-dimensional numerical analysis on seismic behavior of soil-piled raft-structure system. Structures. 2020; 28:905-22. Elsevier.
[35] Deb P, Pal SK. Analysis of load sharing response and prediction of interaction behaviour in piled raft foundation. Arabian Journal for Science and Engineering. 2019; 44:8527-43.
[36] Deb P, Debnath B, Reang RB, Pal SK. Structural analysis of piled raft foundation in soft soil: an experimental simulation and parametric study with numerical method. Ocean Engineering. 2022; 261:112139.
[37] Kumar A, Choudhury D. Development of new prediction model for capacity of combined pile-raft foundations. Computers and Geotechnics. 2018; 97:62-8.
[38] Lee S, Moon JS. Effect of interactions between piled raft components and soil on behavior of piled raft foundation. KSCE Journal of Civil Engineering. 2017; 21:243-52.

[39] Samanta M, Bhowmik R. 3D numerical analysis of piled raft foundation in stone column improved soft soil. International Journal of Geotechnical Engineering. 2019; 13(5):474-83.
[40] Deb P, Pal SK. Structural and geotechnical aspects of piled raft foundation through numerical analysis. Marine Georesources & Geotechnology. 2022; 40(7):823-46.
[41] Bekki H, Tali B, Canou J, Dupla JC. Effect of cyclic loading at a large number of cycles on the bearing capacity of piles in sand. Acta Geotechnica. 2024; 19(2):591-604.
[42] Tarenia K, Patra NR, Rajesh S, Mondal A. Long-term response of piled-raft foundations subjected to incremental compressive loads. Arabian Journal for Science and Engineering. 2024; 49(4):5785-816.
[43] Roh Y, Kim I, Kim G, Lee J. Comparative analysis of axial load capacity for piled-raft foundation with changes in groundwater level. KSCE Journal of Civil Engineering. 2019; 23:4250-8.
[44] Soares WC, Coutinho RQ, Pinto DCR. Piled raft with hollow auger piles founded in a Brazilian granular deposit. Canadian Geotechnical Journal. 2015; 52(8):1005-22.
[45] Das B, Saha R, Haldar S. Effect of in-situ variability of soil on seismic design of piled raft supported structure incorporating dynamic soil-structure-interaction. Soil Dynamics and Earthquake Engineering. 2016; 84:251-68.
[46] http://130.149.89.49:2080/v2016/pdf_books/CAE.pdf, Accessed 30 July 2024.
[47] Helwany S. Applied soil mechanics with ABAQUS applications. John Wiley & Sons; 2007.
[48] Bowles JE, Guo Y. Foundation analysis and design. New York: McGraw-hill; 1996.
[49] Reul O, Randolph MF. Design strategies for piled rafts subjected to nonuniform vertical loading. Journal of Geotechnical and Geoenvironmental Engineering. 2004; 130(1):1-13.
[50] Lee J, Kim Y, Jeong S. Three-dimensional analysis of bearing behavior of piled raft on soft clay. Computers and Geotechnics. 2010; 37(1-2):103-14.
[51] BIS (bureau of Indian standards). Concrete piles, section 4: precast concrete piles in prebored holes (first revision). Indian standard for design and construction of pile foundations–code of practice, IS 2911 part 1. 2010 New Delhi, India: BIS.

Gyan Garima Singh received her B. Tech. degree in Civil Engineering (CE) from Regional Engineering College Bijnor in 2015 and M. Tech. from NIT Hamirpur in 2019. She is pursuing a Ph.D. at MNNIT Allahabad, Prayagraj India. In the Ph.D. thesis, her work is related to Piled raft foundation behaviour under various loading conditions. Her professional and research interests include Foundation, soil behaviour under various loadings, etc.
Email: gyan.2020rce05@mnnit.ac.in

Prof. R.P. Tiwari received B.E. (Civil) from M.N.N.I.T. Allahabad, M.E.(Civil) Geotechnical Engineering from M.N.N.I.T. Allahabad, and Ph.D. degree in Civil Engineering from M.N.N.I.T. Allahabad. Currently he is working as Professor in Civil Engineering department M.N.N.I.T. Allahabad. His area of research is in Soil Mechanics, Foundation Engineering, Rock Mechanics, GIS and Remote Sensing Application. He is professional member of many societies and Life Member of Indian Geotechnical Society, member Indian Road Congress, Member of International Society for Soil Mechanics and Foundation Engineering and many more. He guided many Ph.D., M. Tech degrees in the area of Soil mechanics.
Email: rpt@mnnit.ac.in

Dr. Vijay Kumar received B. Sc. Engineering from M. I. T. Muzaffarpur, Bihar, 2008, M. Tech. from M. N. N. I. T. Allahabad, Prayagraj, 2010, and Ph. D. from M. N. N. I. T. Allahabad, Prayagraj, 2015. Currently he is working as Assistant Professor in Civil Engineering department M.N.N.I.T. Allahabad. His area of research is in Soil Mechanics, Foundation Engineering, Rock Mechanics, Computational Applications in Geotechnical Engineering (Neuro-Fuzzy, ANN & ANFIS). He is the life member of Indian Geotechnical Society, Indian Road Congress, Indian Society for Earthquake Technology, and many more. He guided one Ph.D., and many M. Tech degrees in the area of Soil mechanics.
Email: vkr@mnnit.ac.in

Appendix I

S. No.	Abbreviation	Description
1	k_{rs}	Raft to Soil Stiffness Ratio
2	E_r	Elastic Modulus of Raft
3	B	Raft Width
4	b	Inner Raft Width
5	t_r	Raft Thickness
6	ϑ_s	Poisson's Ratio of Soil
7	ϑ_r	Poisson's Ratio of Raft
8	E_s	Elastic Modulus of Soil
9	L_r	Raft Length
10	n	Number of Piles
11	f_{ck}	Characteristic Strength of Concrete
12	γ	Unit Weight
13	ϑ	Poisson's Ratio
14	ϕ	Angle of Internal Friction
15	δ	Angle of Dilatancy
16	c	Cohesion Yield Stress
17	e	Absolute Plastic Strain
18	S_{avg}	Average Settlement
19	S_{center}	Central Settlement
20	S_{corner}	Corner Settlement
21	S_{diff}	Differential Settlement
22	R_{inter}	Interface Friction

23	W_g/W_r	Pile Group to Raft Width Ratio
24	λ_{avg}	Average Settlement Ratio
25	λ_{diff}	Differential Settlement Ratio
26	2D	Two-Dimensional
27	3D	Three-Dimensional
28	CAE	Complete Abaqus Environment
29	D	Pile Diameter
30	E	Modulus of Elasticity
31	FEA	Finite Element Analysis
32	FE	Finite Element
33	HPRF	Helical Piled Raft Foundation
34	L/D	Length to Diameter Ratio
35	PRF	Piled Raft Foundation
36	SSI	Soil-Structure Interaction
37	S/D	Spacing to Diameter Ratio